



SPE/ISRM 47371

## Reservoir-Scale Fracture Permeability in the Dixie Valley, Nevada, Geothermal Field

C.A. Barton, Stanford University; S.H. Hickman, R. Morin, U. S. Geological Survey; M.D. Zoback, Stanford University; and D. Benolt, Oxbow Geothermal Corp.

Copyright 1998, Society of Petroleum Engineers, Inc.

This paper was prepared for presentation at SPE/ISRM Eurock '98 held in Trondheim, Norway, 8-10 July 1998.

This paper was selected for presentation by an SPE Program Committee following review of information contained in an abstract submitted by the author(s). Contents of the paper, as presented, have not been reviewed by the Society of Petroleum Engineers and are subject to correction by the author(s). The material, as presented, does not necessarily reflect any position of the Society of Petroleum Engineers, its officers, or members. Papers presented at SPE meetings are subject to publication review by Editorial Committees of the Society of Petroleum Engineers. Electronic reproduction, distribution, or storage of any part of this paper for commercial purposes without the written consent of the Society of Petroleum Engineers is prohibited. Permission to reproduce in print is restricted to an abstract of not more than 300 words; illustrations may not be copied. The abstract must contain conspicuous acknowledgment of where and by whom the paper was presented. Write Librarian, SPE, P.O. Box 833836, Richardson, TX 75083-3836, U.S.A., fax 01-972-952-9435.

### Abstract

Borehole televiwer, temperature, and flowmeter data recorded in six wells penetrating a geothermal reservoir associated with the Stillwater fault zone in Dixie Valley, Nevada, were used to investigate the relationship between reservoir permeability and the contemporary in situ stress field. Data from wells drilled into productive and nonproductive segments of the Stillwater fault zone indicate that permeability in all wells is dominated by a relatively small number of fractures striking parallel to the local trend of the fault. However, Coulomb failure analysis using our fracture orientations in conjunction with stress orientations and magnitudes determined by Ref. 1 suggests that fault zone permeability is high only when individual fractures as well as the overall Stillwater fault zone are optimally oriented and critically stressed for frictional failure. Fracture geometry may also play a significant role in determining reservoir productivity. The well-developed populations of low-angle fractures present in wells drilled into the producing segment of the fault are not present within the relatively impermeable segment of the Stillwater fault zone.

### Introduction

The Dixie Valley Geothermal Field is a fault-controlled geothermal reservoir located in the Basin and Range Province of the western United States. The Stillwater fault, a basin bounding normal fault, is the producing reservoir for a geothermal plant operated by Oxbow Geothermal Corporation. However, there are well-documented lateral variations in productivity along the fault that are not fully understood.

Ref. 1, Ref. 2 and Ref. 3 introduce the project background and study objectives, and review the results of previous studies. This paper presents the most recent results of our analysis of the fractured-rock hydrology within and outside the producing reservoir at Dixie Valley. The data discussed herein represents an ongoing integrated study of the relationship between crustal fluid flow and the contemporary in situ stress field.

### Data Acquisition and Analysis

The initial fieldwork for our study was completed in the fall of 1995 when we obtained data from well 73B-7, drilled 2640 m into the producing segment of the Stillwater fault. The remaining fieldwork for this study was completed during an extensive reservoir-scale open-hole logging program from October 1996 through April 1997. In this second phase of fieldwork we obtained sets of borehole televiwer (BHTV), precision temperature, and spinner flowmeter logs from two additional wells within the primary zone of geothermal production (transmissivities on the order of  $1 \text{ m}^2/\text{min}$ ) and from three wells within a few km of the producing zone that were relatively impermeable and, hence, not commercially viable (transmissivities of about  $10^{-4} \text{ m}^2/\text{min}$ ). Using these logs, we have located and oriented faults and fractures and studied their hydrologic properties through comparison with fracture-related thermal and flow anomalies. The measurements made in these wells provide complete data for a systematic, comparative study of the effects of in situ stress on fracture permeability along producing and nonproducing segments of the fault.

Wellbore image data acquisition required an extended field program to cope with the hostile logging conditions of the wells (up to  $240^\circ\text{C}$  temperatures and 3,300 m depths). The Stanford and USGS high-temperature borehole televiwers were used to log these wells. Fundamentals of the operation of these acoustic tools are described in detail in Ref. 4. The strike, dip, and apparent aperture of the fractures have been measured using the digital BHTV analysis system developed at Stanford University<sup>5</sup>.

To date, we have digitized and analyzed approximately 2,887 meters of analog BHTV data recorded in the six wells. The depth intervals over which image data were recorded for this study are presented in Table I (see well location map in

Ref. 1). The digital data were calibrated using numerous field calibration checks conducted before and after each logging run according to our standard field procedure. The data were then processed and edited for systematic noise and other tool-related problems. An example of the BHTV data obtained in well 37-33 is shown in Fig. 1a, where several natural fractures (represented as sinusoids) cross-cut the borehole.

### Fracture Analysis Results

Macroscopic fractures are pervasive throughout the logged interval of each of the wells. Analysis of wellbore image data recorded in each well yields a dominant natural fracture population that is parallel to the local trend of the Stillwater fault.

The orientations of all fractures within the producing reservoir are shown in a lower hemisphere stereographic projection of contoured poles to fracture planes (Fig. 2, after Ref. 6; contour interval = 2.0 sigma). The fracture populations measured in wells drilled along the producing segment of the Stillwater fault have significant scatter in orientation but fractures generally become steeper and larger in apparent aperture with depth. The dominant fracture strike is north to northeast with shallow to moderate dips to the east or west (Fig. 2). The local orientation of the Stillwater fault<sup>7</sup> is shown for reference as the large hachured circles in these diagrams. There are statistical differences in the orientation of these macroscopic fracture populations measured within the producing field and those measured in nonproducing wells to the southwest. Wells drilled into the relatively impermeable segments of the Stillwater fault located 8 and 20 km southwest of the main reservoir show well-developed sets of moderate to steeply dipping fractures. In contrast to the fracture populations measured in wells drilled into the producing fault segments, however, the nonproductive wells have no significant population of low-angle fractures (see Fig. 2, wells 66-21 and 45-14). The lack of low-angle fractures in these wells may impede fracture connectivity with the reservoir.

### Fracture and Fluid Flow Analysis Results

Precision temperature and spinner flowmeter logs (referred to as TPS logs) were acquired in the five additional boreholes of this study in the same manner they were recorded in well 73B-7<sup>3</sup> to provide comparable data sets for all wells. TPS tests were conducted with and without simultaneously injecting water into the well. Fluid flow into or out of individual fractures and faults was determined through analyses of these temperature and spinner flowmeter logs<sup>8</sup>. When a borehole is close to thermal equilibrium with the surrounding rock, heat transfer occurs primarily by thermal conduction and the temperature gradient in the borehole is a function of thermal conductivity and heat flux. Localized perturbations to wellbore temperature will result from localized fluid flow into or out of the borehole and can be detected by precision temperature logging. Fractures or faults that correlate in depth

with these localized temperature perturbations are therefore considered to be hydraulically conductive. Multi-pass temperature logs at various pumping rates allow us to assess the persistence of these detected flow horizons.

The depth locations of individual flow anomalies detected in each of the study wells were established through a combined analysis of temperature profiles, temperature gradient profiles, and spinner logs. Data from multiple passes of the TPS logs were evaluated to determine variations in fluid flow anomalies with changes in pumping rates. The higher fluid production rates in wells 74-7, 73B-7, and 37-33 enhanced the fluid flow anomalies observed in these wells, making them more prominent than anomalies in wells 62-21, 66-21, and 45-14. However, it was possible to determine the zones of fluid movement in the nonproductive wells utilizing the TPS data from several repeat log runs.

The fracture and fluid flow analysis indicates that in both the producing and nonproducing wells there are relatively few fractures that dominate flow. Fig. 3 shows the strike direction of the significant permeable fractures for each of the study wells along with the orientation of the least horizontal principal stress from Ref. 1.

The populations of highly permeable fractures from wells penetrating the producing segment of the Stillwater fault (wells 73B-7, 74-7, and 37-33) clearly define a distinct subset of the total fracture population in each well that is normal to the local direction of the least horizontal principal stress,  $S_{\text{min}}$ . Well 62-21, located in the center of Dixie Valley about 4 km away from wells 73B-7 and 74-7, was drilled to a total depth of 3560 m and did not intersect the Stillwater fault. As discussed by Ref. 1, no in situ stress direction indicators were detected in this well. However, if the stress orientations determined in nearby wells 73B-7 and 74-7 are representative of stresses near well 62-21, then the distinct subset of the overall fracture population in this well that is hydraulically conductive strikes perpendicular to the direction of  $S_{\text{min}}$  (see Fig. 3). Similarly, although cooling crack orientations from well 37-33 were too scattered to yield a reliable stress direction<sup>1</sup>, stress directions from wells 73B-7 and 74-7 (which are located about 5 km to the southwest) suggest that permeable fractures in this well may also be approximately perpendicular to the local direction of  $S_{\text{min}}$ .

As shown in Fig. 3 the populations of relatively permeable fractures in wells 66-21 and 45-14 are somewhat different from the permeable fracture populations observed in the other wells. The more permeable fractures in well 66-21 generally strike in a more easterly direction than do the highly permeable fractures in the producing wells 37-33, 73B-7 and 74-7 but they are still approximately perpendicular to the local orientation of  $S_{\text{min}}$ . In well 66-21, however, the population of permeable fractures is not distinct from the overall northeast trend of all fractures in this well (cf. Fig. 2). The orientations of relatively permeable fractures in well 45-14 are unusual in that they exhibit more scatter than in the other wells and are not related in any simple way to the local direction of  $S_{\text{min}}$ .

**Coulomb Failure**  
By utilizing re-  
measurements an-  
wells<sup>1</sup> we have de-  
faults in these six  
As in the preced-  
assumed to be col-  
to these fractures,  
in situ principal st-  
be known. The she-  
-  $P_1$ ) acting on ea-  
principal stress  
orientation of the  
by Ref. 10, in cor-  
acting on each of  
log from the study  
measured magni-  
formation fluid pr-

Although the  
constrained in the  
known. However,  
producing wells p  
(see Ref. 1), indic-  
this analysis of th-  
zone we assumed  
( $S_{\text{min}} + S_V)/2$ . Fo-  
shear and effecti-  
range of  $S_{\text{Hmax}}$  ma-  
not a particular f-  
relatively insensit-  
by Ref. 1, the pre-  
and 66-21 provi-  
outside the produ-  
zone, with the m-  
segments of the fa-  
frictional analysi-  
(drilled into the  
therefore assumed  
 $S_{\text{Hmax}}$  magnitudes.  
pressures encount-  
Coulomb failure ar-

Using the stres-  
these wells togeth-  
BHTV logs, we ca-  
of the fracture pla-  
to determine whe-  
active fault. Bas-  
frictional strength  
fractures with a  
optimally oriented  
analysis was perfo-  
hydraulically cond-  
producing segmen-  
The results of  
diagrams of shear

### Coulomb Failure Analysis

By utilizing results from hydraulic fracturing stress measurements and observations of wellbore failure in these wells, we have determined the proximity of the fractures and faults in these six wells to Coulomb (i.e., frictional failure). As in the preceding analysis<sup>3</sup>, these fracture planes are assumed to be cohesionless. To apply the Coulomb criterion to these fractures, the orientations and magnitudes of the three in situ principal stresses and the formation fluid pressure must be known. The shear stress and effective normal stress (i.e.,  $S_p - P_p$ ) acting on each fracture plane are then functions of the principal stress magnitudes, the fluid pressure, and the orientation of the fracture plane with respect to the orientations of the principal stresses (see Ref. 9). As discussed by Ref. 10, in computing the shear and effective normal stress acting on each of the fracture planes observed in the BHTV log from the study wells, we used linear approximations to the measured magnitudes of the three principal stresses and the formation fluid pressure.

Although the magnitudes of  $S_{hmin}$ ,  $S_v$ , and  $P_p$  are well constrained in these wells, the magnitude of  $S_{Hmax}$  is poorly known. However, the absence of wellbore breakouts in the producing wells places an upper bound on  $S_{Hmax}$  magnitude (see Ref. 1), indicating that  $S_{hmin} \leq S_{Hmax} \leq S_v$ . Therefore, in this analysis of the fracture data from wells in the producing zone we assumed that  $S_{Hmax}$  at any given depth is equal to  $(S_{hmin} + S_v)/2$ . For wells 73-B, 74-7, and 37-33 computing shear and effective normal stress over the full admissible range of  $S_{Hmax}$  magnitudes, however, shows that whether or not a particular fracture is critically stressed for failure is relatively insensitive to the assumed  $S_{Hmax}$  value. As discussed by Ref. 1, the presence of wellbore breakouts in wells 45-14 and 66-21 provides strong evidence that  $S_{Hmax}$  is higher outside the producing zone than it is within the production zone, with the magnitude of  $S_{Hmax}$  along the nonproducing segments of the fault being greater than or equal to  $S_v$ . For our frictional analysis of fractures in wells 45-14 and 66-21 (drilled into the nonproductive segment of the fault) we therefore assumed  $S_{Hmax} = S_v$  to account for these elevated  $S_{Hmax}$  magnitudes. We also used estimates of the artesian fluid pressures encountered in the nonproductive wells for this Coulomb failure analysis.

Using the stress orientations and magnitudes measured in these wells together with fracture orientations obtained from BHTV logs, we calculated the shear and normal stress on each of the fracture planes and used the Coulomb failure criterion to determine whether or not each plane was a potentially active fault. Based upon laboratory measurement of the frictional strength of prefractured rock<sup>11</sup>, we assumed that fractures with a ratio of shear to normal stress  $\geq 0.6$  are optimally oriented to the stress field for frictional failure. This analysis was performed for all fractures and for the subsets of hydraulically conductive fractures both within and outside the producing segment of the fault.

The results of this analysis are depicted as 3-D Mohr diagrams of shear versus effective normal stress (see Ref. 9)

for the hydraulically conductive fractures in the producing and nonproducing wells (Fig. 4). The great majority of hydraulically conductive fractures encountered within the producing segment of the Stillwater fault zone—as well as the Stillwater fault zone itself (hachured circles)—lie between the Coulomb failure lines for  $\mu = 0.6$  and  $\mu = 1.0$  (Fig. 4, left column); this indicates that these features and the overall Stillwater fault zone are critically stressed, potentially active faults in frictional equilibrium with the current in situ stress field at Dixie Valley. Although drilled near the center of Dixie Valley at a perpendicular distance of several kilometers from the productive segment of the Stillwater fault, well 62-21 exhibits a similar—but less pronounced—tendency for the relatively permeable fractures to be critically stressed failure planes (Fig. 4).

Conversely, many of the hydraulically conductive fractures in the nonproductive wells 66-21 and 45-14 lie below the  $\mu = 0.6$  Coulomb failure curve (Fig. 4, right column) and therefore do not appear to be critically stressed shear fractures. Based on the local stress orientations and magnitudes measured in wells 66-21 and 45-14<sup>1</sup>, the shear and normal stress on the Stillwater fault zone in proximity to these wells (shown as the large hachured circles in Fig. 4) fall below the  $\mu = 0.6$  Coulomb failure line, indicating that the overall fault zone is not critically stressed for frictional failure. In particular, note that the Mohr circle for well 66-21 shows that all fractures are either tangent to or below the  $\mu = 0.6$  Coulomb failure line, suggesting that there is an insufficient ratio of shear to normal stress at this location to promote slip, even on well-oriented fracture planes.

As discussed by Ref. 1, the Stillwater fault zone in proximity to well 45-14 is severely misoriented (by about 41°) for normal faulting in the current stress field. Thus, the ratio of shear to effective normal stress acting on the fault will be highly sensitive to the local magnitude of  $S_{Hmax}$ . As  $S_{Hmax}$  is greater than or equal to  $S_v$  at this location, the Stillwater fault zone falls below the critical value for frictional failure, even though a number of small-scale hydraulically conductive fractures in well 45-14 are critically stressed (Fig. 4).

### Conclusions

We have collected and analyzed fracture and fluid flow data from wells both within and outside the producing geothermal reservoir at Dixie Valley. Data from wellbore imaging and flow tests in wells outside the producing field that are not sufficiently hydraulically connected to the reservoir to be of commercial value provide both the necessary control group of fracture populations and an opportunity to test the concepts proposed in this study on a regional, whole-reservoir scale.

Results of our analysis indicate that fracture zones with high measured permeabilities within the producing segment of the fault are parallel to the local trend of the Stillwater fault and are optimally oriented and critically stressed for frictional failure in the overall east-southeast extensional stress regime measured at the site.

In contrast, in the nonproducing (i.e., relatively

impermeable) well 66-21 the higher ratio of  $S_{hmin}$  to  $S_y$  acts to decrease the shear stress available to drive fault slip. Thus, although many of the fractures at this site (like the Stillwater fault itself) are optimally oriented for normal faulting they are not critically stressed for frictional failure.

Although some of the fractures observed in the nonproducing well 45-14 are critically stressed for frictional failure, the Stillwater fault zone itself is frictionally stable. Thus, the high horizontal differential stress (i.e.,  $S_{Hmax} - S_{hmin}$ ) together with the severe misorientation of the Stillwater fault zone for normal faulting at this location appear to dominate the overall potential for fluid flow.

#### Acknowledgments

This work is supported by the U.S. Department of Energy (DOE) Geothermal Technologies Program. However, any opinions, findings, conclusions, or recommendations expressed herein are those of the authors and do not necessarily reflect the views of the DOE. Additional support was supplied by the Stanford University Department of Geophysics and by GeoMechanics International, Inc.

#### References

- Hickman, S., Zoback, M.D., and Benoit, R.: "Tectonic Controls On Fracture Permeability in a Geothermal Reservoir at Dixie Valley, Nevada", paper SPE 47213, *Proc. Eurock '98*, Trondheim, Norway, (1998) (in press).
- Hickman, S., Barton, C.A., Zoback, M.D., Morin, Sass, J., and Benoit, R.: "In Situ Stress and Fracture Permeability in a Fault-Hosted Geothermal Reservoir at Dixie Valley, Nevada," *Trans. Geothermal Resources Council*, 21, Burlingame, CA, pp. 181-189 (1997).
- Barton, C.A., Hickman, S., Morin, R., Zoback, M.D., Finkbeiner, T., Sass, J., and Benoit, R.: "In-Situ Stress And Fracture Permeability Along The Stillwater Fault Zone, Dixie Valley, Nevada", In: *Proc., Twenty-Second Workshop on Geothermal Reservoir Engineering, SGP-TR-156*, Stanford University, Stanford, California (1997).
- Zemanek, J., Glenn, E.E., Norton, L.J., and Caldwell, R.L.: "Formation Evaluation by Inspection with the Borehole Televiewer", *Geophysics*, (1970) 35, 254.
- Barton, C.A., Tesler, L.G., and Zoback, M.D.: "Interactive Analysis of Borehole Televiewer Data", in *Automated pattern analysis in petroleum exploration*, edited by I. Palaz and S. Sengupta, (1991) Springer-Verlag, 217.
- Kamb, W. B.: "Ice Petrofabric Observations From Blue Glacier, Washington, in Relation to Theory and Experiment", *J. Geophys. Res.*, (1959) 64, 1891.
- Okaya, D.A. and Thompson, G.A.: "Geometry of Cenozoic Extensional Faulting, Dixie Valley, Nevada," *Tectonics*, (1985) 4, 107.
- Paillet, F.L. and Ollila, P.: "Identification, Characterization, and Analysis of Hydraulically Conductive Fractures in Granitic Basement Rocks, Millville, Massachusetts", *Water Resources Investigations, U.S.G.S., WRI* (1994) 94-4185.
- Jaeger, J.C. and Cook, N.G.W.: *Fundamentals of Rock Mechanics* (Third Edition); Chapman and Hall, New York (1979) pp. 28-30.
- Barton, C.A., Zoback, M.D., and Moos, D.: "Fluid Flow Along Potentially Active Faults in Crystalline Rock", *Geology*, (1995) 23, 8, 683.
- Byerlee, J.: "Friction of rocks", *Pure and Applied Geophysics*, (1978) 116, 615.

WELL NAME	DEPTH INTERVAL meters	FRACTURE POPULATION
73B-7	1850-2640	n = 653
74-7	2590-2740	n = 49
37-33	2624-2826	n = 694
62-21	2600-3330	n = 672
66-21	2200-2770	n = 1213
45-14	2280-2725	n = 1264

: "Fluid Flow Along  
the Rock", *Geology*.

Applied Geophysics.

POPULATION  
MEASURED

FRACTURE  
POPULATION

n = 653

n = 49

n = 694

n = 672

n = 1213

n = 1264

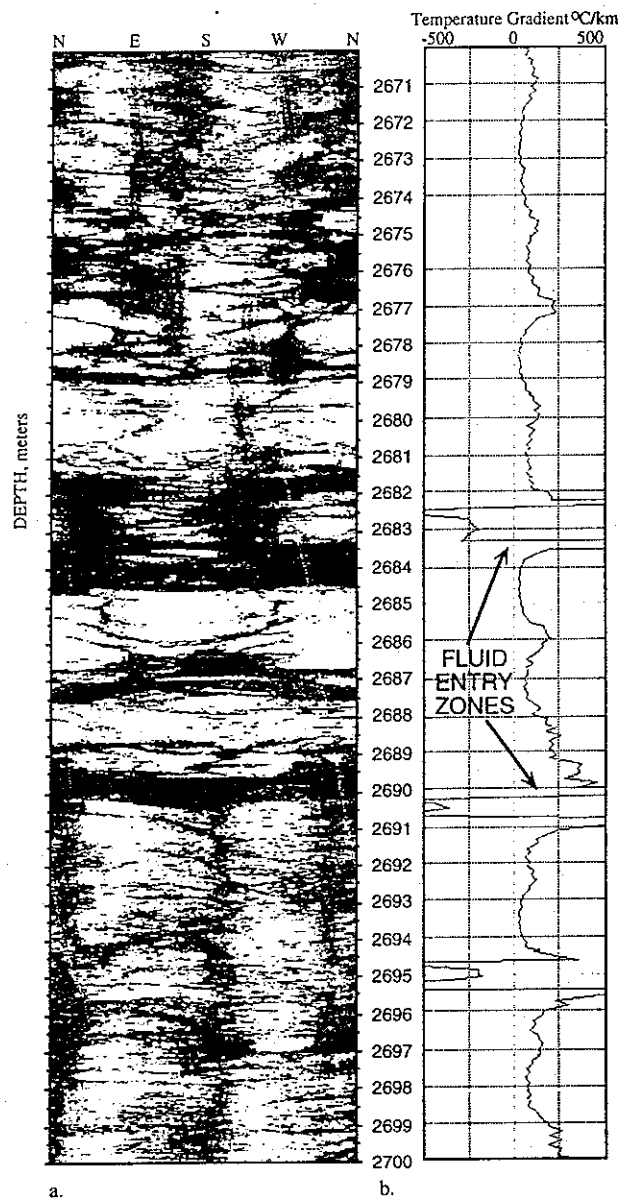


Fig. 1a.—High-temperature borehole televiewer data recorded over the interval 2670–2700 m in well 37-33 located in the producing reservoir at Dixie Valley correlated with temperature gradient data recorded over the same interval (Fig. 1b).

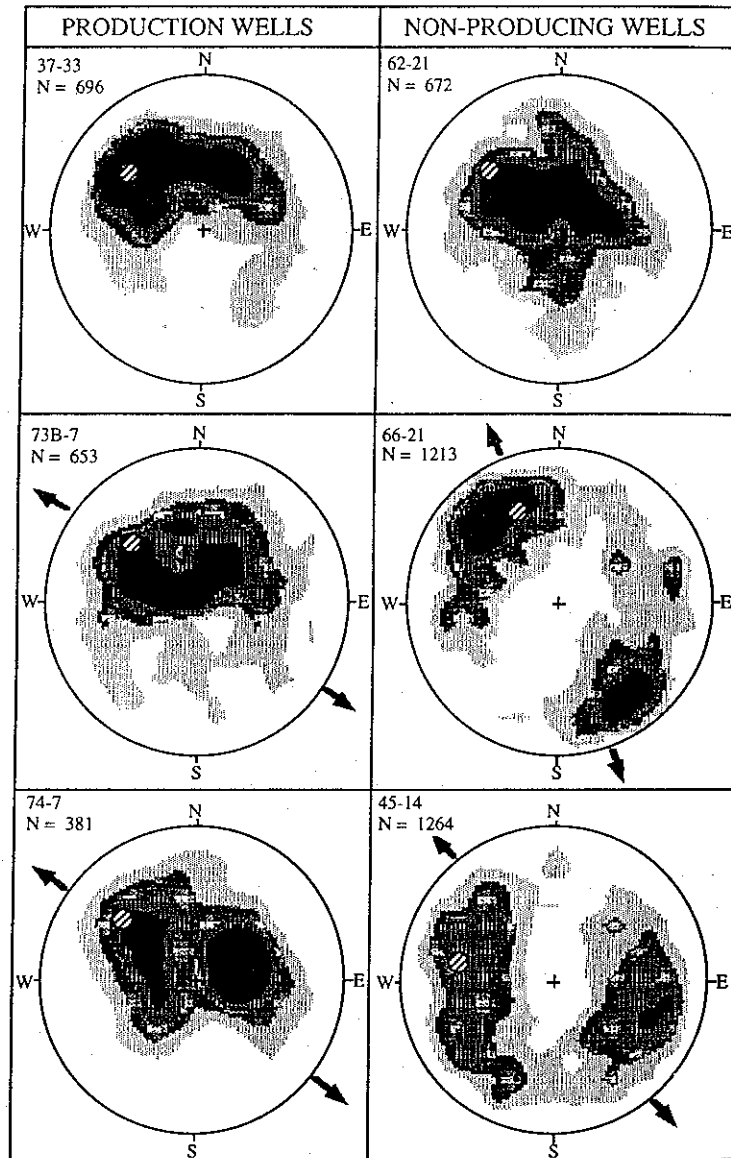


Fig. 2—Kamb contours of poles to fracture planes for producing (left column) and nonproducing (right column) wells in Dixie Valley. The high permeability wells 37-33, 73B-7 and 74-7 and the low permeability wells 66-21 and 45-14 penetrated the Stillwater fault zone at depths of 2-3 km, whereas well 62-21, which failed to encounter permeability to be commercially viable, was drilled adjacent to the permeable segment of the Stillwater fault zone but in the center of Dixie Valley (see location map in Ref. 1). Hachured circles represent poles to the local trend of the Stillwater fault adjacent to each study well. Arrows indicate the orientation of  $S_{\min}$  measured in each well by Ref. 1.

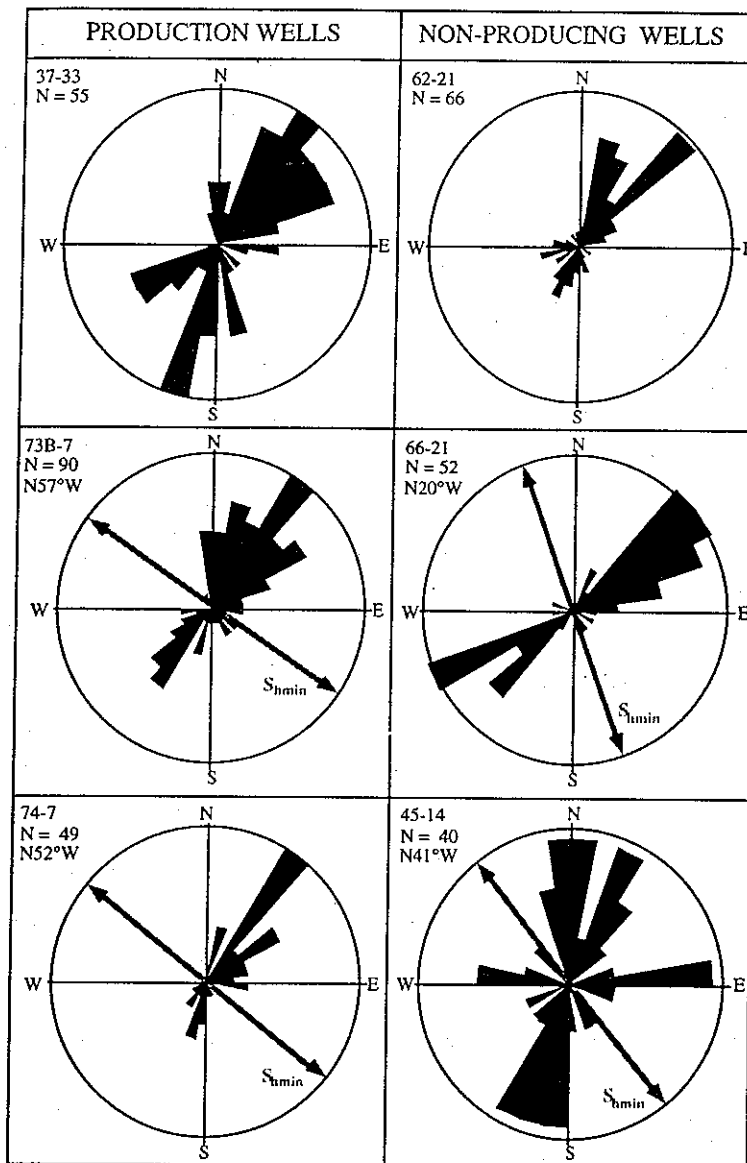


Fig. 3—Histograms showing the subset of fractures from Fig. 2 that are hydraulically conductive from the producing (left column) and nonproducing (right column) wells at Dixie Valley. The orientation of  $S_{min}$  is from Ref. 1.

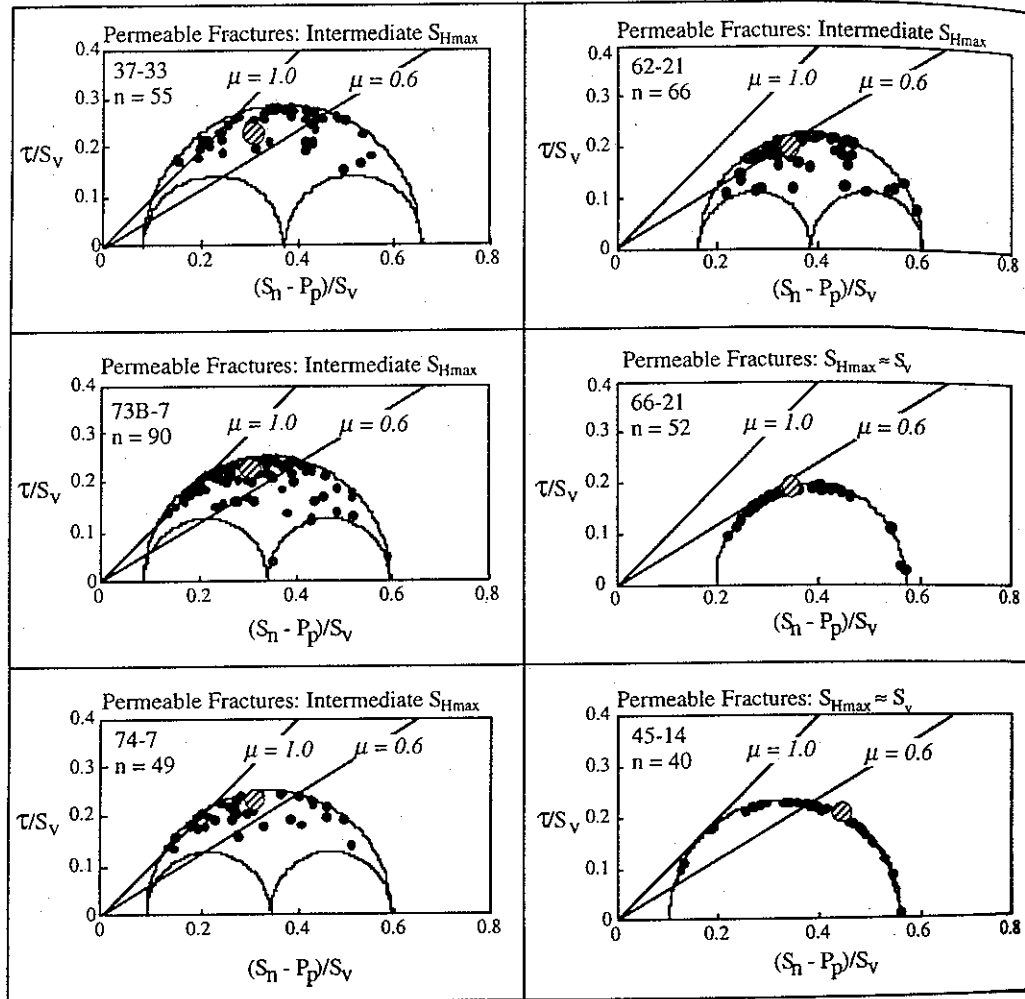


Fig. 4—Normalized shear versus effective normal stress for hydraulically conductive fractures in the producing (left column) and nonproducing (right column) wells (refer to Ref. 9, p. 28, for details of construction of these diagrams). Large hachured circles represent the shear and normal stresses for the Stillwater fault in proximity to each of the study wells.

SPE/ISRI

Laborator  
Zone Stre  
Oedra  
Laboratory), a

August 1998, Socie

to paper was prep  
1998, 1-10 July 199to paper was select  
ation concerned  
ment, have not b  
ation by the aut  
of the Society  
of Engineers, a  
to commercial purpos  
Permissio  
with illustratio  
development of w  
to SPE, Richards

Abstract

temperature z  
length and f  
near fracture  
under fixed co  
pressures (10 t  
to 80°C) to i  
conditions, ro  
how the first i  
diverted temp  
low results im  
and rock stres  
temporating  
considering t  
temperature w

The effec  
parameters m  
depth of bur  
10°C, after v  
fluid pressure  
temperatures,  
displacement  
above a fault  
pressures), b  
to the fract

Productio  
flowing wit